Dynamic Mass Redistribution as a Means to Measure and Differentiate Signaling via Opioid and Cannabinoid Receptors

Ellen E. Codd,[*] John R. Mabus,[†] Brian S. Murray,[‡] Sui-Po Zhang,[§] and Christopher M. Flores[**]

Johnson & Johnson Pharmaceutical Research & Development, Spring House, Pennsylvania.
[*]Present address: Blue Bell, Pennsylvania.
[†]Present address: Centocor Biologics Research, Radnor, Pennsylvania.
[‡]Present address: MedFocus/GlaxoSmithKline, King of Prussia, Pennsylvania.
[§]Present address: Johnson & Johnson Pharmaceutical Research & Development, Radnor, Pennsylvania.
[**]Present address: Johnson & Johnson Pharmaceutical Research & Development, Titusville, New Jersey.

ABSTRACT

Classically, G protein-coupled receptor activation by a ligand has been viewed as producing a defined response such as activation of a G protein, activation or inhibition of adenylyl cyclase, or stimulation of phospholipase C and/or alteration in calcium flux. Newer concepts of ligand-directed signaling recognize that different ligands, ostensibly acting at the same receptors, may induce different downstream effects, complicating the selection of a screening assay. Dynamic mass redistribution (DMR), a label-free technology that uses light to measure ligand-induced changes in the mass of cells proximate to the biosensor, provides an integrated cellular response comprising multiple pathways and cellular events. Using DMR, signals induced by opioid or cannabinoid agonists in cells transfected with these receptors were blocked by pharmacologically appropriate receptor antagonists as well as by pertussis toxin. Differences among compounds in relative potencies at DMR versus ligand-stimulated GTPγS or receptor binding endpoints, suggesting functional selectivity, were observed. Preliminary evidence indicates that inhibitors of intermediate steps in the cell signaling cascade, such as receptor recycling inhibitors, mitogen-activated protein kinase kinase/p38 mitogen-activated protein kinase inhibitors, or cytoskeletal disruptors, altered or attenuated the cannabinoid-induced response. Notable is the finding that mitogen-activated protein kinase kinase 1/2 inhibitors attenuated signaling induced by the cannabinoid type 2 receptor inverse agonist AM630 but not that stimulated by the agonist CP 55,940. Thus, DMR has the potential to not only identify ligands that activate a given G protein-coupled receptor, but also ascertain the signaling pathways engaged by a specific ligand, making DMR a useful tool in the identification of biased ligands, which may ultimately exhibit improved therapeutic profiles.

INTRODUCTION

Opioid and cannabinoid receptors are seven transmembrane-spanning receptors, whose signaling is thought to be mediated via G_i proteins. Each of these receptor families is comprised of several subtypes, including mu (MOR), delta (DOR), and kappa opioid and cannabinoid type 1 (CB1) and type 2 (CB2) receptors, which subserve numerous neuronal and extraneuronal functions. Because of the importance of these physiological functions, opioid and cannabinoid receptors have repeatedly been the targets of drug discovery programs, aimed variously at the discovery of novel agonists or antagonists or the regulation/modification of the levels of endogenous receptor ligands (*e.g.*, enkephalin or anandamide, respectively). Traditional *in vitro* assays supporting basic research and drug discovery programs quantify a single endpoint in a signaling cascade, such as receptor binding affinity or the potency of a ligand to stimulate GTPγS binding to the G protein or inhibition/activation of downstream effectors such as adenylyl cyclase or phospholipase C.

Current thinking that agonists for a given receptor may differentially affect signaling, such that diverse signaling pathways may be activated by individual ligands, raises the issue of the limited purview of any one traditional assay and indeed the potential that it may not be predictive of the desired effect *in vivo*. To circumvent this limitation, some investigators have engaged two different assays (arachidonic acid release vs. IP accumulation,[1] blockade of opioid tolerance development by JNK vs. GRK,[2] cyclic adenosine

ABBREVIATIONS: AB, assay buffer; CB, cannabinoid receptor; cAMP, cyclic adenosine monophosphate; CHO, Chinese hamster ovary; cpm, counts per minute; DAMGO, [D-Ala^2, N-Me-Phe^4, Gly^5-ol]-Enkephalin; DLT, deltorphin II; DMR, dynamic mass redistribution; DOR, delta opioid receptor; GFX, GF109203x; GTPγS, guanosine 5′-[γ-thio]triphosphate; HEPES, 4-(2-hydroxyethyl)piperazine-1-ethanesulfonic acid; MAPK, mitogen-activated protein kinase; MEK, mitogen-activated protein kinase kinase; MOR, mu opioid receptor; nDMR, negative DMR; pDMR, positive DMR; PKC, protein kinase C; pm, picometers; PMA, 12-O-tetradecanoylphorbol 13-acetate; SPA, scintillation proximity assay; Tris, (hydroxymethyl)aminomethane.

DOI: 10.1089/adt.2010.0347

monophosphate [cAMP] accumulation vs. mitogen-activated protein kinase [MAPK] phosphorylation,[3] ligand-induced receptor endocytosis vs. ligand-induced MAPK activation,[4] or G protein vs. β-arrestin-mediated signaling[5]), selecting molecules identified by one or the other, but not both assays. Another approach to this dilemma is the use of label-free technologies such as optical or impedance systems, approaches that have the potential to more broadly report cell signaling responses than do assays quantifying changes at a single point in a signaling array.[6] Dynamic mass redistribution (DMR), an optical measure obtained with Corning's Epic® instrument, quantifies changes in mass density in the portion of the cell proximate to the biosensor-embedded assay plate.[7] In the present DMR study of opioid and cannabinoid receptors, opioid-induced DMR signaling potencies were compared with those obtained at traditional assay endpoints, revealing both similarities and differences. Further, the study sought to identify the cell signaling components underlying mu opioid agonist and CB2 agonist-induced and inverse agonist-induced DMR, revealing the ability of mitogen-activated protein kinase kinase (MEK) 1/2 inhibitors to alter CB2 inverse agonist but not CB2 agonist signaling. Taken together with the differential potencies of opioid agonists in DMR as compared with GTPγS accumulation and receptor binding, these results suggest the usefulness of DMR in the identification of biased ligands and the pathways through which they differentially signal.

MATERIALS AND METHODS

Chemicals

Radiolabeled compounds were obtained from Perkin Elmer (Boston, MA), $MgCl_2$ and Tris from Fisher (Pittsburgh, PA), sucrose from EM Science (Gibbstown, NJ), pertussis toxin from List Biologic Lab (Campbell, CA), and morphine from Spectrum Pharmaceuticals (Irvine, CA). All other compounds, namely, the ligands and signaling activators and inhibitors, were purchased from Tocris (Ellisville, MO) or Sigma (St. Louis, MO).

The cell lines used were either generated at J&J PRD (MOR Chinese hamster ovary [CHO], DOR C6, and DOR CHO) or purchased from suppliers: CB1 CHO and CB2 CHO Euroscreen/Perkin Elmer; SK-N-SH and CHO, ATCC (Manassas, VA). The culture medium (including fetal bovine serum, penicillin, bovine serum albumin, and G418) was purchased from Cellgro (Manassas, VA) and Glutamax I from Invitrogen (Carlsbad, CA).

Animals

All experimental procedures related to animals were approved by the Institutional Animal Care and Use Committee of J&J PRD and were in accordance with the Guidelines for the Care and Use of Laboratory Animals of the National Research Council and The International Association for the Study of Pain.

Opioid Receptor Binding Assays

These assays were performed essentially as previously described.[8] Male Wistar rats (weighing 150–250 g, VAF; Charles River, Kingston, NY) were killed by cervical dislocation, and their brains removed and placed immediately on dry ice. On the day of the experiment, brains were removed from their −80°C storage and placed in ice-cold Tris HCl buffer (50 mM, pH 7.4). The forebrains were separated from the remainder of the brain by a coronal transection, beginning dorsally at the colliculi and passing ventrally through the midbrain–pontine junction. After dissection, the forebrains were homogenized in Tris buffer in a Teflon®-glass homogenizer. The homogenate was diluted to a concentration of 1 g of forebrain tissue per 80 mL Tris buffer and centrifuged at 39,000×*g* for 10 min. The pellet was resuspended in the same volume of Tris buffer containing 5 mM $MgCl_2$ with several brief pulses from a Polytron homogenizer. This particulate preparation was used for the opioid binding assays. After incubation with 2–3 nM of the DOR selective ligand [^{3}H]-[D-Pen^{2,5}]-Enkephalin or 0.8 nM of the MOR selective ligand [^{3}H]-[D-Ala^2, N-Me-Phe^4, Gly^5-ol]-Enkephalin (DAMGO) at 25°C for 2.5 h in a 96-well plate with total volume of 1 mL, the plate contents were filtered through Wallac filtermat B sheets on a Tomtec 96-well harvester. The filters were rinsed three times with 2 mL of 10 mM HEPES buffer (pH 7.4), and dried in a microwave oven. To each sample area, BetaPlate Scint scintillation fluid (LKB) was added and the resulting radioactivity was quantified on an LKB (Wallac) 1205 BetaPlate liquid scintillation counter. K_d and K_i values were calculated using GraphPad Prism.

Agonist-Stimulated GTPγS Binding Assays

These assays were performed essentially as previously described.[8] Membranes from NG-108 cells endogenously expressing DOR or recombinant mu opioid receptor expressing Chinese hamster ovary cells (CHO-hMOR) recombinantly expressing MOR were purchased from Receptor Biology, Inc. (Baltimore, MD). A vial containing 1 mL of membrane was added to 15 mL cold binding assay buffer (AB) comprised of 50 mM HEPES, pH 7.6, 5 mM $MgCl_2$, 100 mM NaCl, 1 mM dithiothreitol, and 1 mM ethylenediaminetetraacetic acid, homogenized with a Polytron, and centrifuged at 3,000 rpm for 10 min. The supernatant was then centrifuged at 18,000 rpm for 20 min. The pellet was resuspended with a Polytron in 10 mL of AB.

The receptor-containing membranes were preincubated in the AB with wheat germ agglutinin-coated SPA beads (Amersham, Piscataway, NJ) at 25°C for 45 min. The SPA bead-coupled membranes were then incubated with 0.5 nM [^{35}S]GTPγS; each assay well contained 1 mg of SPA beads and 3–5 μg of membrane protein. The basal binding was that taking place in the absence of added test compound, with this unmodulated binding considered as 100% and agonist stimulated binding rising to levels significantly above this value. A range of concentrations of receptor agonists was used to stimulate [^{35}S]GTPγS binding. Both basal and nonspecific binding were tested in the absence of agonist, with the nonspecific binding determination including 10 μM unlabeled GTPγS. Radioactivity was quantified on a Packard TopCount, and the percent stimulation was calculated as:

$$\frac{\text{Test compound cpm} - \text{Nonspecific cpm}}{\text{Basal cpm} - \text{Nonspecific cpm}} \times 100 \qquad (1)$$

EC_{50} values were calculated using GraphPad Prism.

Dynamic Mass Redistribution

The cell lines used were grown in Dulbecco's modified Eagle's media/Nut Mix F-12 with Glutamax I, 10% fetal bovine serum, and 1×pen/strep. The medium for the recombinant cell lines also contained the selection agent, G418 (400 μg/mL). The cells were incubated at 37°C with 5% CO_2 in air.

For the DMR assays, cells were plated on Corning Epic tissue culture-treated, 384-well biosensor-containing assay plates at various densities (*Table 1*). Pertussis toxin, when used, was added after the cells were allowed to attach to the assay plate and remained present until the medium was removed, ~18 h later. On the day of the experiment, each well was washed with 40 μL of AB containing Hanks buffered salt solution, 20 mM HEPES, and 0.1% bovine serum albumin. Then, 40 μL of AB (with or without an inhibitor of some component of cell signaling) was added to each well, and the plate equilibrated for 50 min in the Epic system (Corning Life Sciences, Corning, NY). After the measurement of the baseline signal for nine readings (~7 min), the ligand was added in a 10 μL aliquot, and additional DMR measurements were taken at ~40 s intervals for 5,000 s. The shift from baseline to the first peak, expressed in picometers (pm), was obtained and corrected by subtraction of the pm shift obtained in vehicle-treated wells. The resulting concentration–response relationship was analyzed with GraphPad Prism. Separately, the response to the addition of each inhibitor was also studied after its addition after the 50 min preincubation time.

Table 1. Epic™ Assay Protocol

Step	Parameter	Value	Description
1	Plate cells	40 μL	5,000 CB2 CHO; 10,000 MOR, DOR CHO; 20,000 SK-N-SH, DOR C6
2	Incubate	24–48 h	In cell culture incubator 24 h MOR, DOR, CB2 CHO 48 h SH-N-SH, DOR C6
3	Remove medium Wash	– 2×40 μL	Manually Assay buffer
4	Add assay buffer	40 μL	
5	Place cell containing plates in Epic™ instrument, equilibrate	50 min, 26°C	Load plates with plate handler
6	Place ligand dilution plates in Epic™	50 min, 26°C	Load plates with plate handler
7	Baseline reading	~40 s intervals	For nine readings, ~7 min
8	Add ligand	10 μL	From ligand plate
9	Continue reading	~40 s intervals	5,000 s total

Step Notes

1. Add cells with Thermoscientific Multidrop to Corning cell culture plates for Epic™; allow plates to rest at room temp. for 30 min to allow cells to attach
2. 37°C, 5% CO_2 in air
3. Invert plates to manually remove media; add wash buffer with Bio-Mek FX
4. Bio-Mek FX
5. Epic™
6. Epic™
7. Epic™
8. Epic™ liquid-handling accessory
9. Epic™

CB2, cannabinoid type 2 receptor; CHO, Chinese hamster ovary; DOR, delta opioid receptor; MOR, mu opioid receptor.

RESULTS

Mu and Delta Opioid

Stimulation of MOR- and DOR-expressing CHO cells by their cognate agonists resulted in a time-dependent response, namely, a positive DMR (pDMR) with a peak time of about 4 min after application of the agonist. After that time, the signal declined, the rate and extent of the decline being ligand and cell line dependent. Under the conditions tested, the maximum DMR induced by DAMGO in MOR-expressing CHO cells was ~175 pm, and the maximum deltorphin II-induced signal in DOR expressing CHO cells was ~250 pm (*Fig. 1*). The magnitude of the DMR signal obtained with MOR or DOR agonists in SK-N-SH or with DOR agonists in DOR C6 cells was smaller, ~25–40 pm. The DMR responses were not only time dependent but also concentration dependent, enabling the determination of EC_{50} values. *Table 2* contains the EC_{50} values obtained in four cell lines, three recombinantly expressing MOR (MOR CHO) or DOR (DOR C6 glioma and DOR CHO) and one cell line natively expressing both MOR and DOR (SK-N-SH). Subtype selective agonists exhibited appropriate potencies for the opioid receptor subtype with which they have been associated historically, and both MOR and DOR selective agonists elicited a DMR in SK-N-SH cells.

Importantly, the MOR- and DOR-induced DMR signals obtained were inhibited by MOR and DOR selective antagonists, respectively (*Fig. 2*), with the MOR selective antagonist D-Phe-Cys-Tyr-D-Trp-Orn-Thr-Pen-Thr-NH_2 being ineffective in inhibiting DOR-induced DMR, and the DOR selective antagonist H-Tyr-Tic psi [CH_2NH] Phe-Phe-OH being an ineffective inhibitor of MOR-induced DMR (*Table 3*). Some other antagonists such as naltrindole, generally thought of as DOR subtype selective, did not exhibit robust subtype selectivity at the DMR endpoint (*Table 3*). When studied in the absence of an agonist, MOR and DOR antagonists generally produced a very weak pDMR (about 10 pm) that was not dose orderly or that increased slightly at higher concentrations, but in a nontime orderly manner (data not shown).

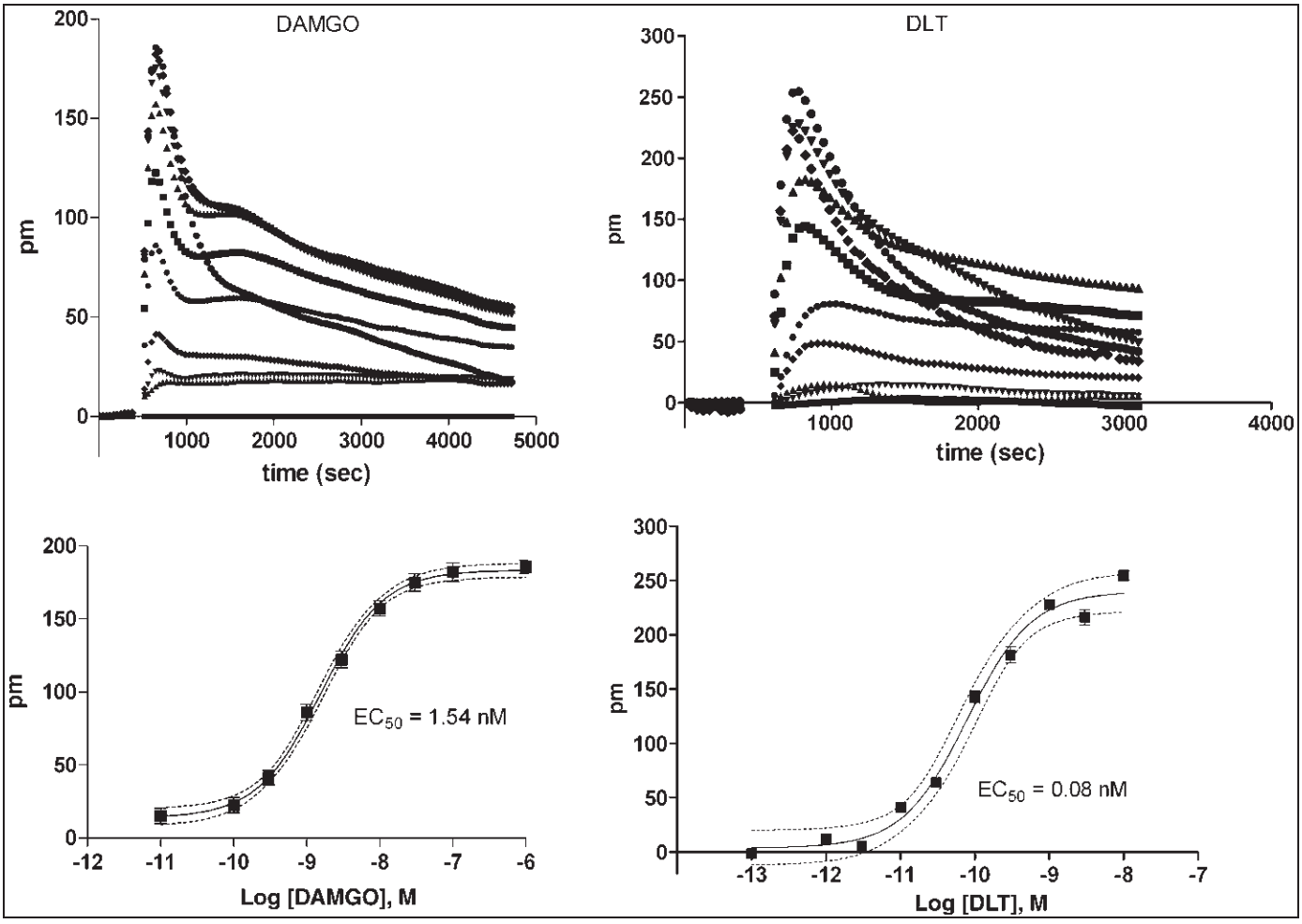

Fig. 1. DAMGO and DLT induced positive DMR in MOR and delta opioid receptor-expressing CHO cells, respectively. The upper panels are the mean DMR tracings obtained before and after addition of the agonist to the assay plate. The lower panels show the concentration–response relationship obtained using the peak response at 3–5 min after ligand addition. The values shown are the means ± SEM of replicate determinations (24 for DAMGO and 8 for DLT) at each concentration. The resulting nonlinear regressions of the concentration response curves are shown with their 95% CL and well as their EC_{50} values. CHO, Chinese hamster ovary; DAMGO, [D-Ala^2, N-Me-Phe^4, Gly^5-ol]-Enkephalin; DLT, deltorphin II; DMR, dynamic mass redistribution; MOR, mu opioid receptor.

Comparison of the DMR potencies with the potencies of the same compounds in the GTPγS assay and with MOR binding affinities revealed differences in the potency order at the various endpoints (*Fig. 3*). For all compounds tested, the binding affinity was the smallest of the three values obtained, and most compounds were ~10-fold more potent at the DMR endpoint than in the GTPγS functional assay. However, the DMR potency of DAMGO was virtually identical to the compound's binding affinity, whereas for d-propoxyphene, DMR was the weakest of the three endpoints measured. These potency differences at diverse assay endpoints suggest divergence in signaling or functional selectivity among the agonists tested.

To better understand the signaling pathways underlying the MOR agonist-induced DMR signal, activators and inhibitors thought to interact with various cell signaling pathways were used. Administered alone, the cAMP activator forskolin induced a concentration-dependent negative DMR (nDMR, *Table 4A*), with a potency of 7 nM and a maximum signal of approximately −150 pm. In the presence of a maximally stimulating concentration of forskolin (30 nM), DAMGO concentration dependently reversed the forskolin-induced nDMR, reaching a maximum pDMR similar to that obtained in the absence of forskolin, ~200 pm. The DAMGO potency was unchanged by forskolin, with EC_{50} values of 3.0 nM in the presence and 3.5 nM in the absence of forskolin, when evaluated concurrently (*Table 4A*).

In the same MOR-expressing CHO cells, the protein kinase C (PKC) activator PMA but not the inactive phorbol 4α-phorbol 12,13-didecanoate induced a pDMR, with a potency of 13 nM (*Table 4A*). Further, the PMA-induced DMR was blocked by the PKC inhibitor

Table 2. Dynamic Mass Redistribution Potency of Opioid Agonists in Cells That Express Mu Opioid Receptor and Delta Opioid Receptor

Agonist	DMR EC_{50} (nM)			
	MOR CHO	SK-N-SH	DOR C6	DOR CHO
DAMGO	1.54	3.0	>1,000	695
Hydromorphone	3.7	3.3	–	–
Morphine	33.4	55.9	–	–
Oxycodone	112	268	–	–
D-propoxyphene	1,294	491	–	–
Deltorphin II	–	0.1	3	0.08
[D-$Pen^{2,5}$]-Enkephalin	>1,000	0.4	4.4	0.09
SNC80	–	–	13.9	–

Concentration–response studies were conducted in four cell lines expressing MOR, DOR, or both receptors. Each study contained 8–10 ligand concentrations with 8–24 replicates at each concentration.

DAMGO, [D-Ala^2, N-Me-Phe^4, Gly^5-ol]-Enkephalin; DMR, dynamic mass redistribution.

GF109203x (GFX), pointing to a PKC role in the signal. In parallel studies, however, morphine-induced DMR was not attenuated by GFX (*Table 4B*), suggesting that PKC is not involved in the morphine-induced DMR in the present experiments. Neither the protein kinase A inhibitor H89 nor the MEK 1/2 inhibitor U0126 altered the morphine-induced DMR (*Table 4B*). None of the cell signaling inhibitors used (*i.e.*, GFX, H89 or U0126) induced a positive or a negative DMR when tested alone in the MOR CHO cells (*Table 4B*). Importantly, both MOR and DOR induced DMR were fully blocked by preincubation of MOR CHO and DOR CHO cells with pertussis toxin (*Table 4B*), demonstrating the $G_{i/o}$ dependence of the MOR- and DOR-mediated DMR. *Figure 7* illustrates hypothetical cellular interactions for many of the ligands, activators, and inhibitors used in this study.

Cannabinoid

Stimulation of CB2-expressing CHO cells by CB2 agonists resulted in a pDMR with a peak time of 8 min, whereas stimulation by a CB2 inverse agonist provoked a negative DMR (*Fig. 4*). The CB2 agonist CP 55,940 exhibited a potency of 1.7 nM and a maximum pDMR of ~110 pm, whereas the CB2 inverse agonist AM 630 exhibited a potency of 18 nM and a maximum nDMR of approximately −80 pm. Importantly, signaling induced by the agonist CP 55,940 was concentration dependently blocked by AM 630. *Table 5* shows the potency and maximum DMR signal induced by some established CB2 ligands. Neither CP 55,940 nor AM 630 induced a significant response in parental, non-CB2-transfected CHO cells.

To better understand the cell biology underlying the CB2-induced DMR, studies were undertaken using various agents thought to interfere with discrete steps in cell signaling. These studies probed both the agonist-induced and inverse agonist-induced DMR to better understand the differences, if any, in their signal transduction processes. Pretreatment with pertussis toxin blocked the DMR induced by both CP 55,940 and AM 630 (*Fig. 5*), suggesting that the signaling induced by both the agonist and inverse agonist was $G_{i/o}$ dependent. The cytoskeletal disruptor latrunculin A concentration dependently reduced both CP 55,940-induced and AM 630-induced DMR (*Table 6*), achieving a full block at 1 μM, whereas the PI3K inhibitor wortmannin, across the concentration range of 0.1–1,000 nM, slightly enhanced both agonist and inverse agonist signaling. At no concentration tested (1–10,000 nM) did the p38 MAPK inhibitor SB 202190 alter either CP 55,940 or AM 630 induced signaling (*Table 6*), whereas a differential effect on CP 55,940 and AM 630 provoked signaling was effected by the MEK 1/2 inhibitor U0126 (*Table 6*, *Fig. 6*). At concentrations from 1 to 1,000 nM U0126, no concentration-dependent change in the CP 55,940-induced DMR was observed, whereas the MEK 1/2 inhibitor U0126 concentration dependently reduced the nDMR induced by AM 630, fully blocking the signal at a U0126 concentration of 1 μM (*Fig. 6*). The effects of the MEK 1/2 inhibitor SL327 recapitulated those of U0126, having no effect on CP 55,940-induced signaling, but concentration dependently and fully blocking the nDMR induced by AM 630 (*Table 6*). When added to the cells after the preincubation/stabilization time and without any added CB2 agonist or inverse agonist, U0126 itself induced an nDMR similar to that provoked by AM630, suggesting that it had cell signaling effects analogous to those of a CB2 inverse agonist. The diagram in *Figure 7* illustrates hypothetical interrelationships among many of the ligands, activators, and inhibitors used in this study.

DISCUSSION

Opioid Signaling

When evaluated via DMR, the mu and delta opioid pharmacology of the compounds tested generally confirmed the findings obtained with classical assay methods: canonical ligands exhibited appropriate receptor selectivity (mu vs. delta), antagonists concentration dependently reduced the signaling of agonists, and signaling was blocked by preincubation with pertussis toxin. Differences, however, between DMR and GTPγS potencies or alterations in the order of potencies of the opioid ligands in the various assays suggest functional diversity at these signaling endpoints. One possibility is that signaling events other than or in addition to GTPγS accumulation may contribute to the DMR signal. These signaling components could include the βγ G protein subunits,[9] a non-$G_{i/o}$ G protein such as G_z[10,11] or G_s,[12,13] or non-G protein mediated signaling, such as that transduced via β-arrestin.[14,15] However, the abolition of the DMR signal by pretreatment of the cells with pertussis toxin suggests that the DMR signal studied here is $G_{\alpha i}/G_{\alpha o}$ dependent.

Another explanation for differences in potencies at the endpoints measured is the different nature of the DMR and GTPγS signals:

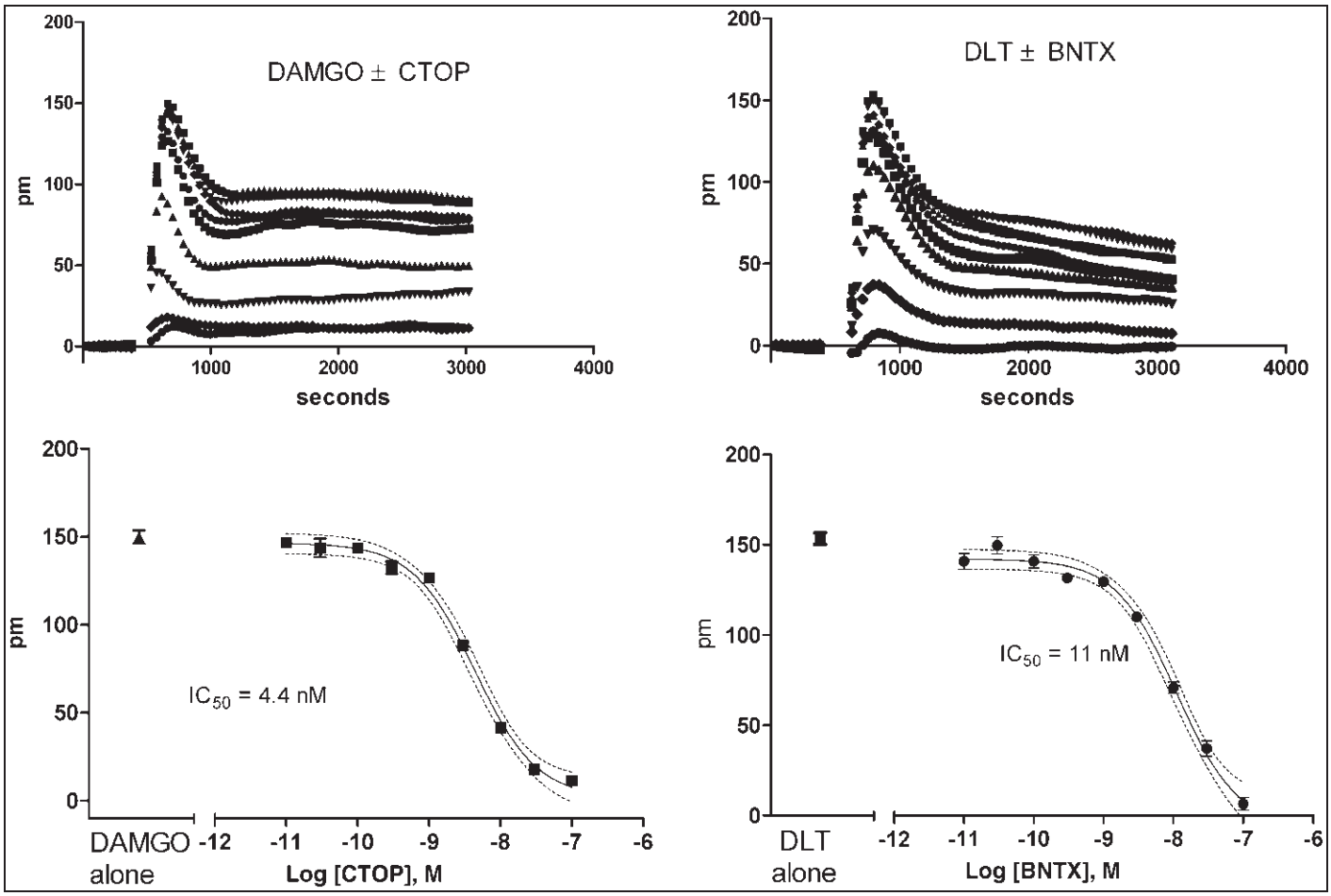

Fig. 2. Appropriate antagonists inhibited DAMGO (3 nM)-induced and DLT (0.3 nM)-induced DMR in CHO cells expressing MOR or delta opioid receptor, respectively. The upper panels are the mean DMR tracings obtained before and after addition of the agonist to each well in the assay plate, the antagonists having been added to the plate previously with the AB. The lower panels show the concentration–response relationship obtained using the peak response at 3–6 min after ligand addition. Shown are the means ± SEM of 4–8 replicate determinations at each concentration studied. The resulting nonlinear regressions of the concentration–inhibition curves are shown with their 95% CL and well as their IC_{50} values.

rather than being the product of a specific biochemical event, the DMR signal derives from changes in the index of refraction of cellular components within ~150 nm of the surface of the assay plate. Thus, cellular events taking place more distally from the plasma membrane, unless they alter the macro-conformation of the cell, may be invisible events to the Epic biosensor. For example, in the present studies, the MAPK pathway inhibitor U0126 did not reduce morphine-induced DMR, although it has been demonstrated that MAPK phosphorylation is stimulated by MOR activation by its cognate agonists.[16] In the present studies, neither did GFX block morphine-induced signaling, although in astrocytes, it was an effective blocker of mu agonist-induced ERK phosphorylation.[17] Conceivably, at least in MOR-expressing CHO cells, MAPK phosphorylation does not induce changes in mass density detectible within the portion of the cell monitored by the biosensor.

The true lack of involvement of a cellular component in a specific signaling event rather than the mere invisibility of that event to the Epic biosensor can be probed with the use of specific cell signaling activators. In the present studies, the PKC activator PMA induced a pDMR in MOR CHO cells, illustrating the detectability of this signal by the biosensor. Further, this pDMR was inhibited by the PKC inhibitor GFX, demonstrating that the biosensor is also sensitive to the inhibition of signaling at this level of the signaling pathway. Thus, the lack of GFX reduction of morphine-stimulated DMR in the present studies suggests that the morphine-induced signal does not involve a PKC-sensitive step.

Cannabinoid Signaling

When evaluated via DMR, CB2 pharmacology also appeared to be similar to that obtained with classical assay methods: canonical

Table 3. Dynamic Mass Redistribution Inhibitory Potency of Opioid Antagonists in Cells That Express Mu Opioid Receptor and Delta Opioid Receptor

	DMR IC_{50} (nM)			
	vs. 3 nM DAMGO	vs. 3 nM DAMGO/ 1 nM DLT	vs. 0.3 nM DLT	
Antagonist	MOR CHO	SK-N-SH	DOR C6	DOR CHO
7-Benzylidenenaltrexone	18	–	0.3	11
Naltriben	8	–		0.7
Naltrindole	1.6	0.8/0.7	0.7	0.6
SDM25N	513	–	–	30
H-Tyr-Tic ψ $[CH_2NH]$Phe-Phe-OH	4,500	–	–	0.6
D-Phe-Cys-Tyr-D-Trp-Orn-Thr-Pen-Thr-NH_2	4.4	8.2/NT	–	>1,000

Concentration inhibition studies were conducted in four cell lines expressing MOR, DOR, or both receptors. Each study contained 8–10 antagonist concentrations, with 8–24 replicates at each concentration.

NT, not tested.

Table 4. Effect of Activators (A) and Inhibitors (B) of Intracellular Signaling on the Dynamic Mass Redistribution in Mu Opioid Receptor Chinese Hamster Ovary Cells

A.

Activator	Effect of activator alone	Effect of activator on DAMGO stimulated DMR
FK	nDMR, EC_{50} = 7 nM	no effect
PMA	pDMR, EC_{50} = 13 nM	NT
4α-Phorbol 12, 13-didecanoate	No effect	NT

B.

	Inhibitor effect	
Inhibitor	On PMA induced DMR	On DAMGO or morphine stimulated DMR
PTX	NT	Blocked
GF109203x	Inhibited	No effect
H89	NT	No effect
U0126	No effect	No effect

Except when studied alone, the activator or inhibitor was added before the ligand during the equilibration period.

nDMR, negative DMR; NT, not tested; pDMR, positive DMR; PMA, 12-O-tetradecanoylphorbol 13-acetate.

ligands exhibited appropriate receptor selectivity (CB2 vs. CB1, data for the latter not shown), inverse agonists concentration dependently reduced the signaling of agonists, and signaling was blocked by preincubation with pertussis toxin, indicative of $G_{i/o}$ mediation of the DMR signal. Also in keeping with previously published CB2 functional studies was the observation of bidirectional modulation of signaling by agonists and inverse agonists, similar to those observed at GTPγS and MAPK endpoints.[18] Thus, DMR measures of CB2 receptor signaling appear to encompass the pharmacologic profiles derived from classical assays using single probe endpoints.

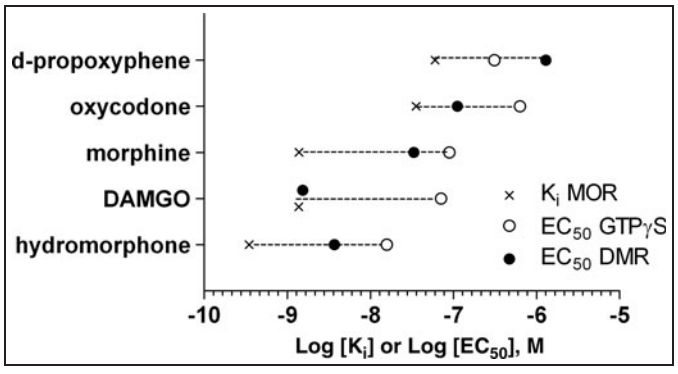

Fig. 3. Comparison of responses of several MOR agonists in three MOR assays assessing binding assessing agonist binding affinity or functional potency. Binding affinity was determined in membranes prepared from rat brain cortex, whereas EC_{50} values were determined in MOR CHO cells (DMR) or membranes from MOR CHO cells (guanosine 5′-[γ-thio]triphosphate). GTPγS, guanosine 5′-[γ-thio]triphosphate.

Pertussis toxin blockade of CB2 agonist signaling has been previously demonstrated at GTPγS binding,[18] MAPK phosphorylation,[18] and cAMP accumulation[19] endpoints; the present work extends these findings for cannabinoid agonists to the DMR endpoint. Of greater importance, however, is the novel finding that pertussis toxin blocks not only agonist but also inverse agonist DMR signaling, a pharmacologic interaction not previously investigated. The finding of a role for the G protein in the function of inverse agonist as well as agonist signaling favors an integrated view of CB2 receptor signaling over categorization into opposing classes such as agonist or inverse agonist. This more integrated view comprises a continuum of receptor efficacy from full agonist to full

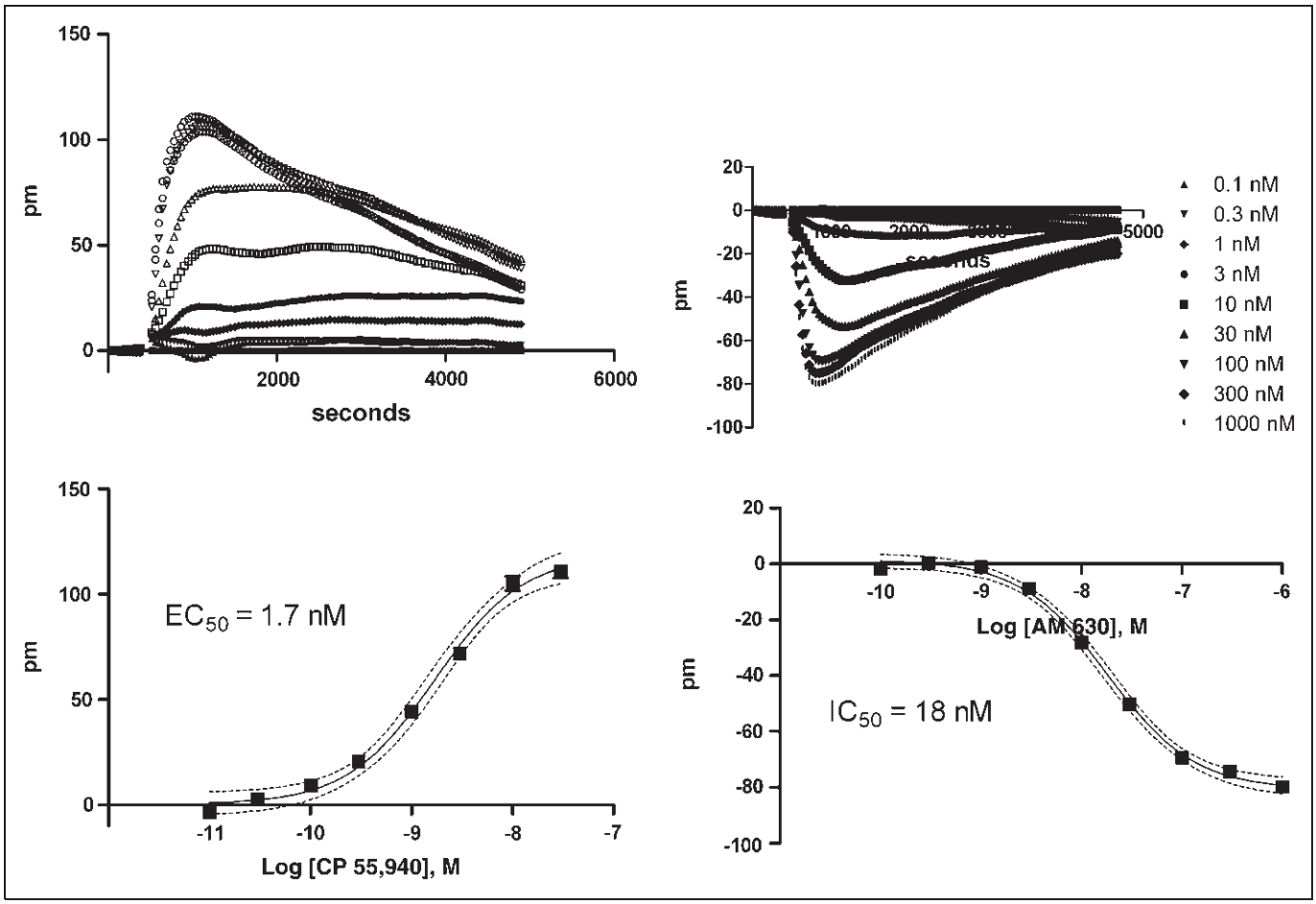

Fig. 4. CP 55,940 and AM 630 induced a positive and a negative DMR, respectively, in CB2 CHO cells. Shown are the mean values of 24 replicate determinations at each concentration studied. The lower panels show the concentration–response relationship obtained using the peak response at 8–9 min after ligand addition. The resulting nonlinear regressions of the concentration–response curves are shown with their 95% CL and well as their EC_{50} values. CB2, cannabinoid type 2 receptor.

inverse agonist, with numerous possible intermediate activation/efficacy states.

Not surprisingly, given the well-established role of basal signaling in CB2 receptor function, experimental approaches to reducing basal signaling have been developed. Chief among these techniques is preincubation of the receptor with an inverse agonist such as SR 144528[20] or AM 630.[21] The present study exploited a novel approach to the modulation of basal signaling, by inhibiting MAPK phosphorylation, shown with both U0126 and SL 327. This approach extends thinking about signaling pathways and the roles of their several components, demonstrating that CB2 cell signaling can be modulated at multiple cellular levels. In fact, the present results are the first demonstration of the use of an MAPK inhibitor, or for that matter of an inhibitor of any downstream cell signaling process, to reduce CB2 basal signaling. This unique approach enabled study of both agonist and inverse agonist signaling, making possible for the

Table 5. Potency and Maximum Effect Obtained in Dynamic Mass Redistribution Assay of Cannabinoid Type 2 Receptor Chinese Hamster Ovary Cells

Compound	DMR EC_{50} (nM)	DMR max (pm)
AM630	18.1	−80
CP 55,940	1.7	129
GW405833	IA	IA
L759656	0.25	130
SR144528	18.0	−44
WIN55212-2	0.29	60

The compounds studied include both agonists and inverse agonists.
IA, not active.

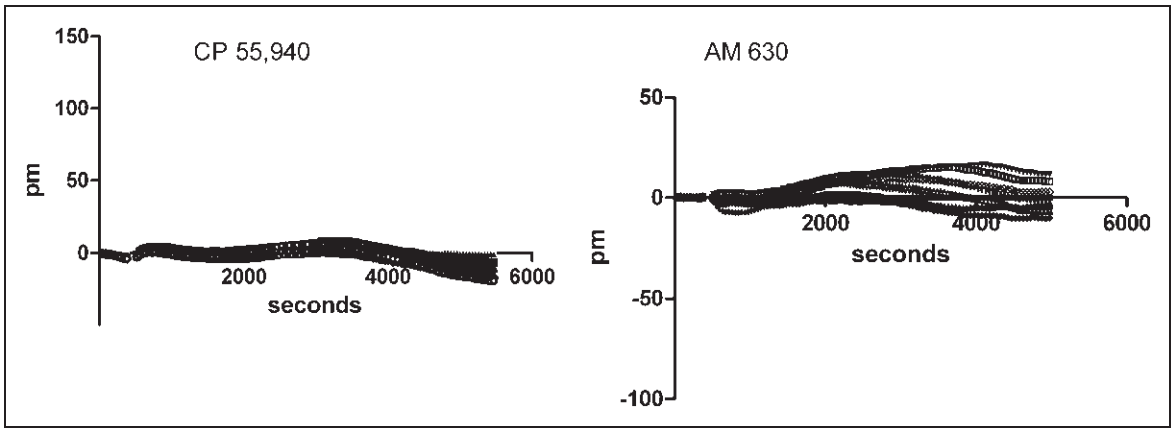

Fig. 5. Pertussis toxin blocked both agonist and inverse agonist DMR signals in CB2 CHO cells. The data shown are the mean values of 12 replicate determinations at each ligand concentration studied (CP 55,740: 0.01–100 nM; AM 630: 0.1–1,000 nM). Samples assayed in parallel without the addition of Pertussis toxin exhibited a robust response similar to that in the upper portion of *Figure 4*.

first time observation of differential effects of the inhibitor on agonist versus inverse agonist signaling.

SUMMARY

The time-responsive nature of the DMR profile affords a broad view not usually provided by assays of cell signaling, which typically report an effect at a specified signaling step and at a particular time point. Certainly, assays can be repeated at several fixed times, yielding some understanding of time as well as concentration effects on the measured response. Of necessity, however, the number of time points investigated is limited by assay considerations. DMR, however, routinely provides detailed spatio-temporal signaling profiles at each activator concentration studied. The present work focuses on cellular events comprising the DMR peak (both positive and negative); future studies will be needed to probe more extensively the signaling events comprising the movement toward baseline (either downward or upward) of the DMR signal.

Further, DMR comprises not only events commonly cataloged as cell signaling activities, but also events taking place remotely (with respect to the receptor) but still dependent on receptor activation, such as cytoskeletal integrity, as evidenced by the reduction and

Table 6. Effect of Inhibitors of Intracellular Signaling on Dynamic Mass Redistribution Induced by CP 55,940 or AM 630 in Cannabinoid Type 2 Receptor Chinese Hamster Ovary Cells

Signaling inhibitor	Postulated cellular interaction	Effect on CP 55,940 DMR signal	Effect on AM 630 DMR signal
Pertussis toxin	ADP ribosylates Giα, thereby blocking Gi/o-mediated signaling	Abolishes DMR	
Latrunculin A	Reversibly disrupts actin cytoskeleton; associates with actin monomers, thereby preventing their repolymerization	Concentration-dependent reduction of DMR; full block at 1 μM	
Wortmannin	PI3K inhibitor; blocks receptor recycling from early endosomes	Slightly greater	
		pDMR	nDMR
U0126	MEK 1/2 inhibitor	No effect on DMR	$IC_{50} = 0.35\ \mu M$
SL327	MEK 1/2 inhibitor	No effect on DMR	$IC_{50} = 17\ \mu M$
SB 202190	Cell-permeable p38 mitogen–activated protein kinase inhibitor	No effect on DMR	

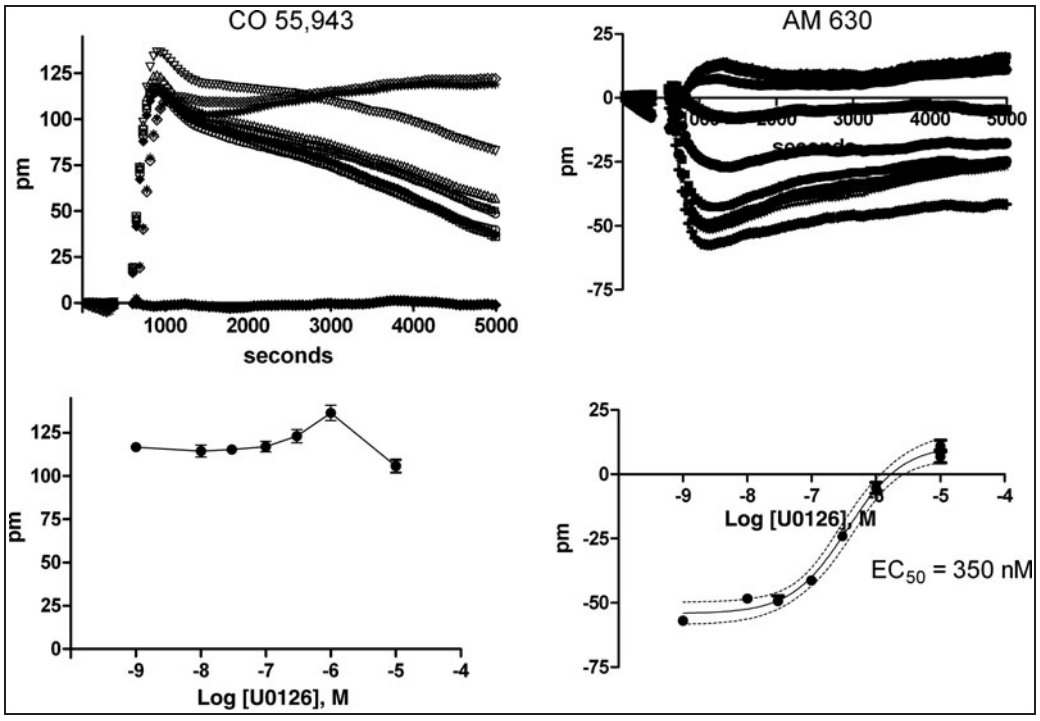

Fig. 6. The MEK 1/2 inhibitor U0126 blocked the DMR induced by AM 630 (300 nM) but not that induced by CP 55,940 (300 nM) in CB2 CHO cells. The values shown are the mean of 12 replicate determinations at each inhibitor concentration (1–10,000 nM). The lower panels show the concentration–response relationship obtained using the peak response at 8–9 min after ligand addition, and where appropriate, the resulting nonlinear regression of the concentration inhibition curve, with its 95% CL and IC_{50} value.

eventual abolition of the CB2 signal by latrunculin A. Thus, DMR has the potential to represent more globally than does any one conventional assay endpoint the spatio-temporal response of the cell to ligand activation (see Kenakin[22]), whether that ligand is an agonist or an inverse agonist, making DMR a powerful tool in the study of pluidimensional cell signaling responses. Used in conjunction with inhibitors of specific signaling pathways, DMR has the potential to select sets of ligands that, although acting at the same receptor, differentially activate downstream pathways.

The ultimate challenge in the study of such biased ligands, however, remains their characterization *in vivo*, that is, the delineation of the diverse pharmacologies that ligands acting at the same receptor but signaling via different downstream pathways mediate. Progress on this front, achieved through the characterization of groups of such molecules in animal models predictive of therapeutic effects, will enable the rational design of (biased) ligands that engage specific signaling pathways to more precisely target desired therapeutic endpoints. These molecules have the potential to precisely alter disease pathology, thus avoiding undesired effects mediated by pathways extraneous to the pathology, as they will be devoid of the latter formerly hidden activities, not seen previously because of molecule selection via assays with a very limited pharmacologic view. Drug candidates having defined constellations of efficacies, measured in texture-rich assays *in vitro*, have a greater chance of clinical therapeutic success due to our broader understanding of their efficacy spectrum and the contribution of that profile to the desired therapeutic phenotype.

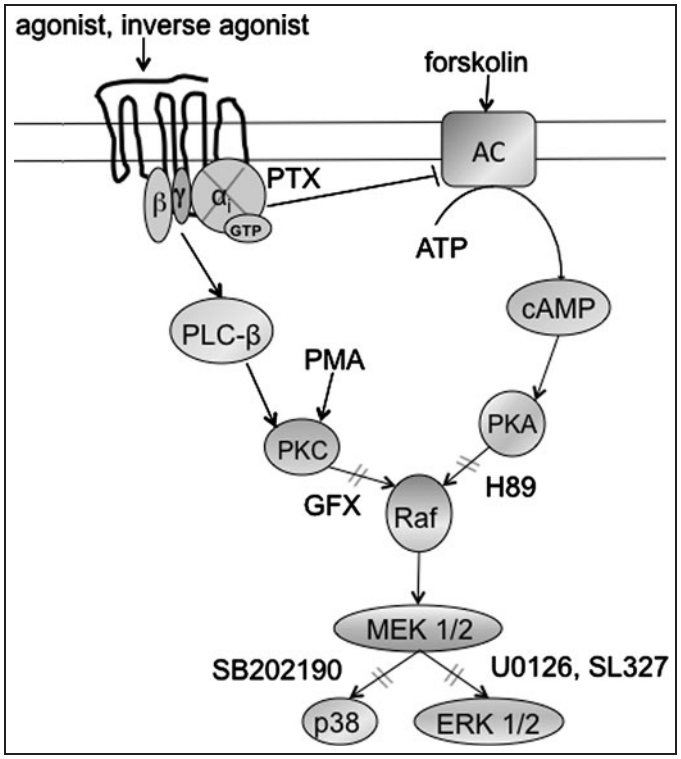

Fig. 7. Diagram of some GPCR signaling pathways. Protein components of cell signaling are shown, as well as some activators and inhibitors of their action.

ACKNOWLEDGMENT

The authors wish to thank Dr. Hong Xin for her expert help with the Epic™ instrument, as well as her thoughtful review of and suggestions on this article.

AUTHOR DISCLOSURE STATEMENT

At the time this work was conducted, the authors were employed by Johnson & Johnson Pharmaceutical Research and Development, LLC.

REFERENCES

1. Berg KA, Maayani S, Goldfarb J, Scaramellini C, Leff P, Clarke WP: Effector pathway-dependent relative efficacy at serotonin type 2A and 2C receptors: evidence for agonist-directed trafficking of receptor stimulus. *Mol Pharmacol* 1998;54:94–104.
2. Melief EJ, Miyatake M, Bruchas MR, Chavkin C: Ligand-directed c-Jun N-terminal kinase activation disrupts opioid receptor signaling. *Proc Natl Acad Sci USA* 2010;107:11608–11613, S11608/11601–S11608/11606.
3. Sato M, Horinouchi T, Hutchinson DS, Evans BA, Summers RJ: Ligand-directed signaling at the beta 3-adrenoceptor produced by 3-(2-ethylphenoxy)-1-[(1,S)-1,2,3,4-tetrahydronaphth-1-ylamino]-2S-2-propanol oxalate (SR59230A) relative to receptor agonists. *Mol Pharmacol* 2007;72:1359–1368.
4. Whistler JL, von Zastrow M: Dissociation of functional roles of dynamin in receptor-mediated endocytosis and mitogenic signal transduction. *J Biol Chem* 1999;274:24575–24578.
5. Violin JD, Lefkowitz RJ: beta-Arrestin-biased ligands at seven-transmembrane receptors. *Trends Pharmacol Sci* 2007;28:416–422.
6. Kenakin T: Interrogating 7TM receptors: does texture in the question yield greater texture in the answer? *J Recept Signal Transduct* 2009;29:132–139.
7. Fang Y, Li G, Peng J: Optical biosensor provides insights for bradykinin B2 receptor signaling in A431 cells. *FEBS Lett* 2005;579:6365–6374.
8. Codd EE, Carson JR, Colburn RW, *et al.*: The novel, orally active, delta opioid RWJ-394674 is biotransformed to the potent Mu opioid RWJ-413216. *J Pharmacol Exp Ther* 2006;318:1273–1279.
9. Mathews JL, Smrcka AV, Bidlack JM: A novel Gbeta gamma -subunit inhibitor selectively modulates mu -opioid-dependent antinociception and attenuates acute morphine-induced antinociceptive tolerance and dependence. *J Neurosci* 2008;28:12183–12189.
10. Hasbi A, Nguyen T, Fan T, *et al.*: Trafficking of preassembled opioid mu -delta heterooligomer-Gz signaling complexes to the plasma membrane: coregulation by agonists. *Biochemistry* 2007;46:12997–13009.
11. Fan T, Varghese G, Nguyen T, Tse R, O'Dowd BF, George SR: A Role for the distal carboxyl tails in generating the novel pharmacology and G protein activation profile of mu and delta opioid receptor hetero-oligomers. *J Biol Chem* 2005; 280:38478–38488.
12. Wang H-Y, Burns LH: Naloxone's pentapeptide binding site on filamin A blocks mu opioid receptor-Gs coupling and CREB activation of acute morphine. *PLoS One* 2009;4:e4282.
13. Wang H-Y, Frankfurt M, Burns LH: High-affinity naloxone binding to filamin A prevents Mu opioid receptor-Gs coupling underlying opioid tolerance and dependence. *PLoS One* 2008;3:e1554.
14. Bohn LM, Dykstra LA, Lefkowitz RJ, Caron MG, Barak LS: Relative opioid efficacy is determined by the complements of the G protein-coupled receptor desensitization machinery. *Mol Pharmacol* 2004;66:106–112.
15. Bohn LM, Gainetdinov RR, Lin FT, Lefkowitz RJ, Caron MG: Mu-opioid receptor desensitization by beta-arrestin-2 determines morphine tolerance but not dependence. *Nature* 2000;408:720–723.
16. Li L-Y, Chang K-J: The stimulatory effect of opioids on mitogen-activated protein kinase in Chinese hamster ovary cells transfected to express mu -opioid receptors. *Mol Pharmacol* 1996;50:599–602.
17. Belcheva MM, Clark AL, Haas PD, *et al.*: Mu and Kappa opioid receptors activate ERK/MAPK via different protein kinase C isoforms and secondary messengers in astrocytes. *J Biol Chem* 2005;280:27662–27669.
18. Bouaboula M, Desnoyer N, Carayon P, Combes T, Casellas P: Gi protein modulation induced by a selective inverse agonist for the peripheral cannabinoid receptor CB2: implication for intracellular signalization cross-regulation. *Mol Pharmacol* 1999;55:473–480.
19. Demuth DG, Molleman A: Cannabinoid signalling. *Life Sci* 2006;78:549–563.
20. Portier M, Rinaldi-Carmona M, Pecceu F, *et al.*: SR 144528, an antagonist for the peripheral cannabinoid receptor that behaves as an inverse agonist. *J Pharmacol Exp Ther* 1999;288:582–589.
21. Mancini I, Brusa R, Quadrato G, *et al.*: Constitutive activity of cannabinoid-2 (CB2) receptors plays an essential role in the protean agonism of (+)AM1241 and L768242. *Br J Pharmacol* 2009;158:382–391.
22. Kenakin TP: Cellular assays as portals to seven-transmembrane receptor-based drug discovery. *Nat Rev Drug Discov* 2009;8:617–626.

Address correspondence to:
Ellen E. Codd
736 Cathcart Road
Blue Bell, PA 19422

E-mail: ellen.codd@verizon.net